



ELSEVIER

Nuclear Instruments and Methods in Physics Research A 418 (1998) 314–321

**NUCLEAR
INSTRUMENTS
& METHODS
IN PHYSICS
RESEARCH**
Section A

The electric field in irradiated silicon detectors

L.J. Beattie, T.J. Brodbeck, A. Chilingarov*, G. Hughes, S.A. McGarry,
P.N. Ratoff, T. Sloan

Department of Physics, University of Lancaster, Lancaster LA1 4YB, UK

Received 20 March 1998; received in revised form 4 June 1998

Abstract

The electric field distribution inside heavily irradiated silicon particle detectors is deduced using observations of α particle and minimum ionising particle signals. In these detectors α particle signals are observed for both p^+ and n^+ side illumination even when the detector is only partially depleted. The observations indicate that the electric field distribution within the partially depleted detector has the contribution expected from a uniform space charge, as in unirradiated detectors, together with a strong, short range, local electric field in the vicinity of the p^+ electrode and a non-zero electric field in the remaining part of the detector. © 1998 Elsevier Science B.V. All rights reserved.

PACS: 07.77-n; 85.30-z

Keywords: Electric field; Irradiated silicon detectors

1. Introduction

The behaviour of unirradiated silicon particle detectors is well understood. If they are illuminated by α particles, signals are observed from the junction side at all voltages whereas they are only observed from the ohmic side at voltages starting from a value which is just below the depletion voltage when the electric field reaches a depth to which the α particles penetrate. In contrast, irradiated detectors behave differently in a manner similar to that observed in more complicated materials such as GaAs [1].

In this paper we describe our observations of α particle signals for illumination from both sides of a heavily irradiated detector as well as those of minimum ionising particles (MIPs) from a β source. We use the data to show that in such detectors there is a similar electric field pattern to that in an unirradiated detector together with an extra local electric field in the vicinity of the p^+ electrode. This extra field is shown to be strong and of short range. We also show that a small non-zero electric field exists in what is usually called the non-depleted region of the detector.

The detector used in all the measurements described here was a standard n-type p-i-n diode of thickness $300\ \mu\text{m}$ irradiated by a fluence of $1.3 \times 10^{14}\ \text{cm}^{-2}$ pions of momentum $300\ \text{MeV}/c$. After irradiation it was left for about a week at

*Corresponding author. Tel.: +44 1524 594627; fax: +44 1524 844037; e-mail: chilinga@lavhep.lancs.ac.uk.

room temperature to allow beneficial annealing [2] to take place. The minimum depletion voltage thus reached was found to be 209 V. The depletion voltage was determined from C–V measurements at 10 kHz and 0°C by the standard method of finding the crossing point of two straight-lines fitting the log C–log V plot in the vicinity of the “kink” in the C–V dependence.

After beneficial annealing the detector was stored at a temperature of $\sim 0^\circ\text{C}$. The measurements described below were made at temperatures between 10°C and 20°C taking care that the detector did not spend more than a few hours at these temperatures to avoid reverse annealing [2]. This detector is one of a sample of 11 similar diodes used for a general study of radiation damage effects in Si. The charge collection results for the detector which are reported here are similar to those observed in the other detectors [3] which were irradiated by fluences of between $1\text{--}3 \times 10^{14} \text{ cm}^{-2}$ pions or neutrons. Hence the data presented here can be regarded as typical for a detector which has been subjected to such irradiation fluences.

2. Signals from α particles in irradiated detectors

As is well known [4] after heavy irradiation the initial n-type silicon becomes p-type. Therefore, the junction moves to the n^+ side of the detector and the depleted region should develop from this side. To investigate this, irradiated detectors were tested with α particles. Surprisingly, signals were observed for p^+ side illumination even at voltages well below the depletion voltage. Fig. 1 shows the α particle signal measured in terms of the charge collection efficiency (CCE) for the irradiated detector described in the present paper for α particles illuminating the n^+ and p^+ sides. The CCE is the ratio of the charge observed in the detector after irradiation to that observed in the same detector before irradiation. The x-axis is expressed in terms of the normalised depletion thickness d discussed in more detail in the following section.

Even at full depletion ($d = 1$) the CCE does not reach 100%. This is due to carrier trapping as discussed in the following sections. The CCE for short range α particles depends strongly on the field

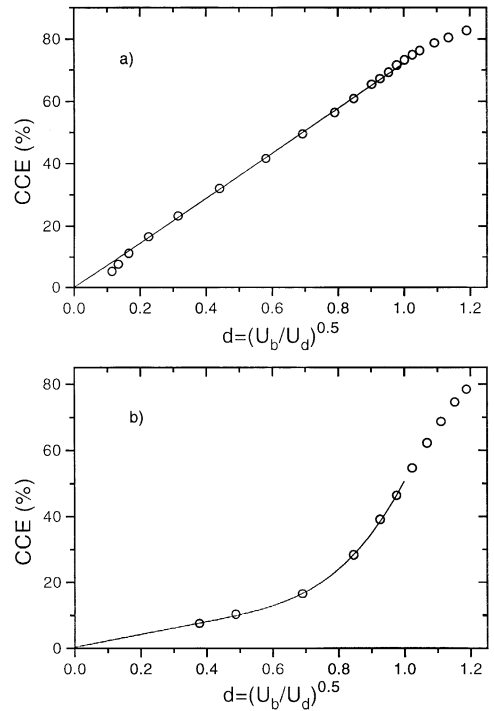


Fig. 1. (a) Charge collection efficiency for α particles as a function of $d = \sqrt{U_b/U_d}$ for n^+ side illumination. The linear fit is discussed in the text. (b) The same for the p^+ side illumination with a smooth curve which is the result of the fit of the model to the data described in the text (see Section 5). The detector was irradiated by a fluence of $1.3 \times 10^{14} \text{ cm}^{-2}$ pions of momentum 300 MeV/c and then annealed to a minimum depletion voltage.

at the side where the ionisation is deposited. Immediately above depletion the field at the p^+ side grows quite quickly with voltage leading to a rapid rise in the CCE above $d = 1$. In contrast, the relative change of the field at the n^+ side is smaller leading to a smaller increase of the CCE for this side.

2.1. α Particle signal from the n^+ side

The measured CCE for n^+ side illumination by α particles was found to vary linearly with the square root of the bias voltage, U_b , up to the depletion voltage, U_d . The simplest explanation of this is as follows.

The depleted region grows proportionally to $\sqrt{U_b}$ as expected for the case of a uniform space

charge in the depleted region. The holes drifting from the n^+ electrode induce their signal directly on the p^+ electrode because, for fast electric signals (characteristic time ~ 10 ns) produced by the hole drift, the non-depleted part of the detector behaves like an insulator. (This follows e.g. from the well-known fact [5] that for frequencies above 100 kHz the value of the capacitance of irradiated detectors is almost independent of voltage.) Since the holes practically stop at the end of the depleted region their induced signal (from Ramo's theorem [6]) is proportional to the ratio d of the depleted region thickness to the total detector thickness. This ratio in turn can be expressed as

$$d = \sqrt{U_b/U_d}. \quad (1)$$

Fig. 1a shows the measured CCE for n^+ side illumination by α particles as a function of d , together with a linear fit to the data through the points below $d = 1$. The lowest three points were omitted from the fit since the drift field in the diode for these points is so low that the plasma effect [7] begins to influence the results. It can be seen that the linear fit gives a good representation of the data.

However, the CCE does not reach 100% at the depletion voltage ($d = 1$) and the loss is ascribed to charge trapping. This loss is expected to be constant with bias below the depletion voltage. This can be understood from the compensation between the increasing drift distance ($x_d \sim \sqrt{U_b}$) and increasing drift velocity of the carriers with increasing bias. The characteristic drift time $t_d = x_d^2/\mu_n U_b$ then remains the same for all values of U_b , hence keeping constant the trapping which depends on the ratio t_d/τ_h . Here μ_n and τ_h are the hole mobility and trapping time constant in the material, respectively.

Below depletion the CCE growth is due to the increase of the drift distance while the collection time remains almost constant. Above depletion the drift distance becomes constant but the collection time decreases with voltage. This leads to a further increase of the CCE due to a decrease in the trapping probability. The fact that in Fig. 1a for a few points above depletion the CCE still grows almost linearly with d is accidental. A detailed analysis of

the CCE dependence on voltage above full depletion is given elsewhere [8].

2.2. α particle signal from the p^+ side

Fig. 1b shows the measured CCE from α particles illuminating the p^+ side of the detector, as a function of the normalized depletion width, d , which is related to the bias voltage by Eq. (1). The signal from the p^+ side for α particles (Fig. 1b) appears when less than 50% of the detector is depleted and then grows smoothly with bias. Such behaviour is very different from unirradiated detectors in which the signal is completely absent until the detector becomes almost fully depleted when the electric field reaches the penetration depth of the α particles. The smooth curve in Fig. 1b is a fit to the data based on the model which is described in Section 5.

The unexpected observation of signals from short range ($\sim 20 \mu\text{m}$) α particle from the p^+ side in irradiated detectors well before the detector is fully depleted shows that there must be an electric field present in such detectors at this side even when the depleted region does not yet reach it. To investigate the strength of this field the time of arrival of the signals from the p^+ side was compared with that from the n^+ side. If the field on the p^+ side is weak the reduced carrier velocity together with the plasma effect [7] will cause a significant delay in the arrival of the signal from this side. Conversely, if the field is strong the delay will be small. Here the plasma effect [7] plays a major role. This effect causes a time delay in the separation of hole-electron pairs because of the neutralisation of the electric field in the vicinity of the ionisation. The induced-time delay due to the plasma effect has been measured to be $\sim 27 \text{ ns}/E$ with the external electric field, E , in kV/cm [8].

The overall delay was measured by comparing the differences of the signal arrival times and the α particle impact times for p^+ and n^+ side α particle illumination of the detector. The time delay between the α particle impact and the signal arrival was measured using α - γ coincidences from an ^{241}Am source. The impact time of the α particle was obtained by detecting the coincident γ -ray in a scintillation counter. The γ signal was used to

start a Time to Amplitude Converter and the α signal to stop it, so that the output amplitude gave a measure of the relative time delay between the α particle impact time as signalled by the γ -ray and the ionisation arrival time. The time spectra were measured for both p^+ and n^+ side α particle illumination.

Fig. 2 shows a typical time spectrum. The events at large delay time arise from random coincidences which populate the whole time range uniformly. The peak corresponds to the real coincidences. The exponential rise up to the peak at small times is due to the fact that the excited $^{237}_{93}\text{Np}$ daughter nucleus from $^{241}_{95}\text{Am}$ decay is an isomeric transition with a mean lifetime of 91 ns [9]. Hence there is an exponential time distribution of the start times ob-

tained from the γ -ray with a sharp fall to the random coincidence count level. This sharp fall corresponds to the earliest arrival time of the γ start signal. All the time spectra taken showed similar shapes to that in Fig. 2. The sharpness of the fall to the random background shows that there is little time smearing of the ionisation as it passes through the detector and this fall time was similar for all the measurements.

To obtain the delay time of the ionisation arrival in the detector a fit of a functional form was performed to each spectrum. This function consisted of a flat (random) background together with an exponential rise up to a fixed time, which was a free parameter, with a Gaussian fall at times greater than this fixed time. The half-maximum point on

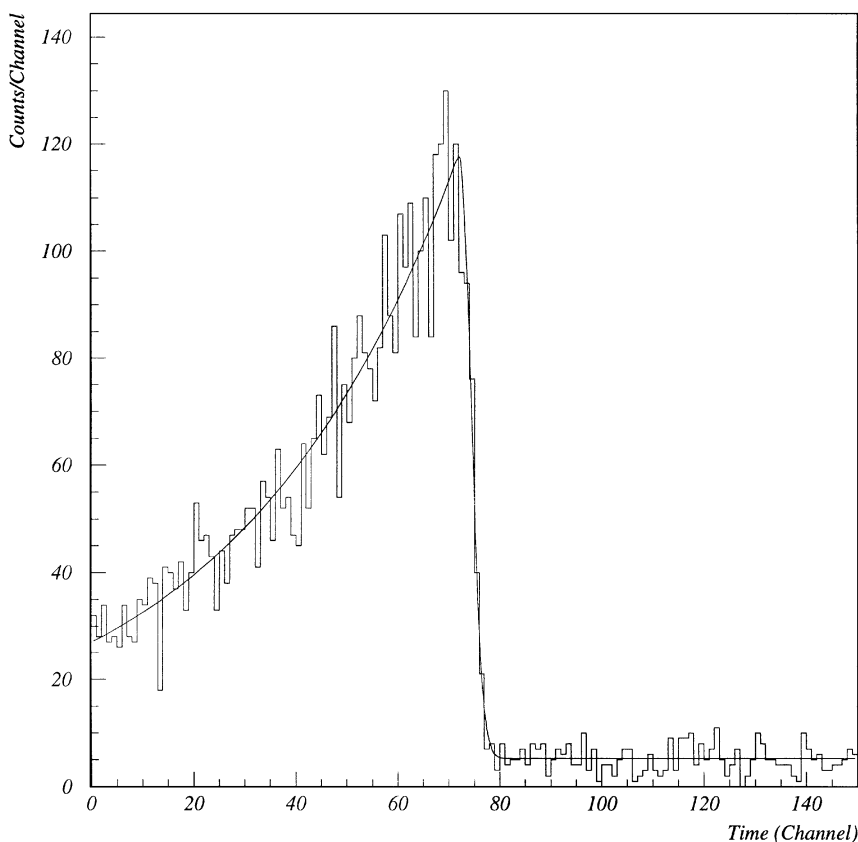


Fig. 2. A typical time difference spectrum between the γ -ray arrival and the arrival of the ionisation from the α particle. The smooth curve is the result of the fit described in the text. For this spectrum the detector was biased at 40 V and illuminated by α particles from the n^+ side. The time calibration is 2.1 ns per channel and the Gaussian σ from the fit is 4.8 ns.

this fall was used to measure the average relative delay of the ionisation arrival time in the detector. Time slewing in the discriminator connected to the detector (which had a fixed threshold) occurred because of the finite risetime (~ 60 ns) of the detector's amplifier. Corrections (up to 15 ns) for this time slewing were made to each spectrum. The correction was obtained by measuring separately the time slewing for large α particle pulses from an unirradiated detector. The ionisation arrival time was measured for different levels of attenuation of these pulses, i.e. for different triggering times in the discriminator. For each spectrum from the irradiated detector the amplitude above threshold was determined and the ionisation arrival time then corrected to a fixed amplitude. The corrected arrival times were measured for both p^+ and n^+ illumination and the difference was taken. Since at the n^+ side the field exists at all bias voltages and is about 2 times higher than the average field in the depleted region, this difference describes the delay

of the signal related to the low field near the p^+ side.

Fig. 3 shows the difference between the signal arrival times for α particles impinging on the p^+ and the n^+ sides as a function of the normalised depletion layer width, d (which is related to the bias voltage by Eq. (1)). The delay time is short (~ 7 ns) and independent of the bias voltage (or depletion layer thickness) within the errors. As mentioned above the plasma delay has been measured to be ~ 27 ns/E with E in kV/cm [8]. For the measured delay time to be as short as ~ 7 ns the electric field in the vicinity of the p^+ electrode must be of the order of several kV/cm i.e. similar in strength to the field in the bulk of the detector. Hence, there must be a rather strong electric field in the vicinity of the p^+ electrode of the detector.

3. Signals from MIPs in irradiated detectors

Signals from MIPs in the irradiated detectors were measured using a collimated β source and a system of scintillation counters to define particles which traverse the whole detector as described in Ref. [10]. Fig. 4 shows the MIP CCE as a function of the detector bias voltage together with a linear fit to the data up to the depletion voltage. This fit

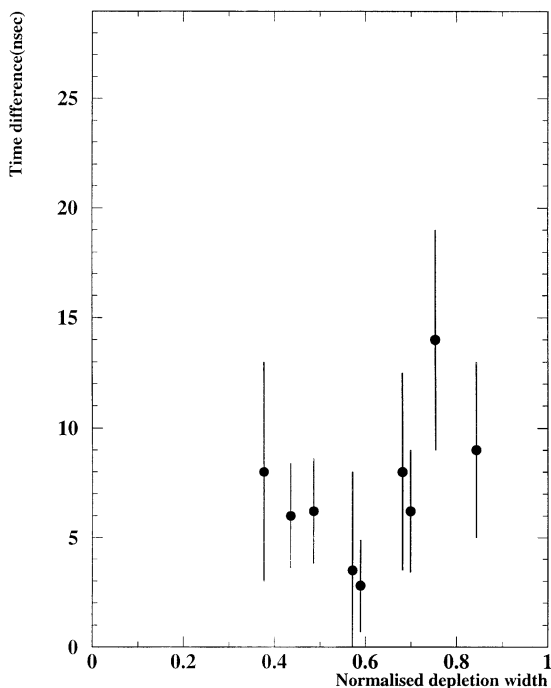


Fig. 3. Difference in the arrival times (in ns) of the α particle signals from the p^+ and n^+ sides as a function of the normalised depletion width $d = \sqrt{U_b/U_d}$.

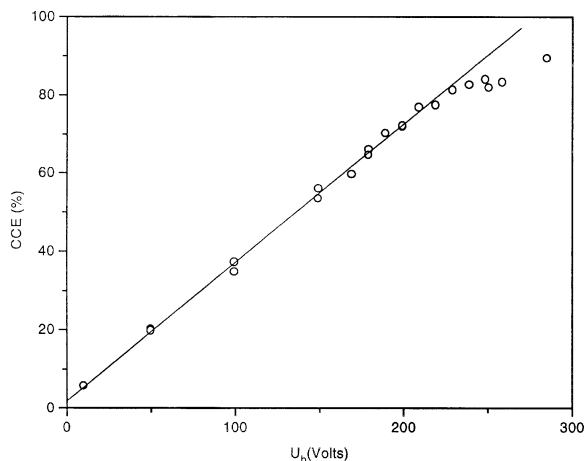


Fig. 4. Measured CCE for MIPs as a function of the bias voltage. The straight line is the linear fit to the data discussed in the text.

gives a good representation of the data showing that the CCE increases linearly with bias.

Such a behaviour can be understood as follows. The deposited ionisation in the active (depleted) region varies linearly with the depletion width. The induced signal per unit ionisation also varies linearly with the depletion width from Ramo's theorem [6], as discussed in Section 2.1. Hence the signal from MIPs which traverse the whole detector will vary as the product of the two effects, i.e. as the square of the depletion width. The behaviour of the detector for n^+ illumination by α particles shows that this depletion width varies as the square root of the bias voltage (see Fig. 1a), hence the signal from MIPs will vary linearly with bias voltage, as observed.

4. The electric field pattern in irradiated detectors

A picture emerges of the electric field distribution in the partially depleted irradiated detectors from all the above information. This field is similar to that for a uniform space charge in the depleted region falling to near zero at the edge of the depleted region. This is necessary to explain the linear

behaviour of the MIP CCE with bias and the linear behaviour of the n^+ α particle CCE with the square root of the bias voltage. However, in order to explain the observation of α signals from the p^+ side which are not significantly delayed there must be a strong local field in the vicinity of the electrode on this side. To explain the smooth variation with voltage of the alpha particle CCE from the p^+ side one needs also a non-zero electric field in the area between the high field region near the p^+ electrode and the depleted region.

Fig. 5 shows a schematic diagram of the electric field pattern in the detector which we deduce from these observations. The width of the high electric field region adjacent to the p^+ side may be quite small.

5. A model for the α particle CCE from the p^+ side

Assuming that the electric field pattern follows the form described in the previous section and shown in Fig. 5, we can develop a model to describe the observed α particle CCEs for illumination from the p^+ side for voltages below the depletion voltage. We should stress that at this stage it is a minimal phenomenological modification of the field structure in a standard semiconductor detector. An analysis of the possible physical origins of such modifications or the development of a more elaborate model will be the subject of future studies.

We start with the assumption of the simplest (i.e. uniform) electric field E_0 in the non-depleted region. We assume further that the strength of this field is linearly related to the thickness of the depleted region (e.g. through the current generated in it, but there may also be other reasons). Therefore, we express the field through the normalised depletion width d (from Eq. (1)), so that $E_0 = dE_{\max}$. Here E_{\max} is the nominal value of E_0 when the detector is fully depleted ($d = 1$). (The word nominal denotes the fact that when E_0 reaches E_{\max} the non-depleted area where E_0 should exist vanishes.) Finally, we introduce the normalised maximum "absorption length", i.e. the carrier mean free path in the electric field E_{\max} . This is given by

$$\lambda = \mu_e E_{\max} \tau_c / w, \quad (2)$$

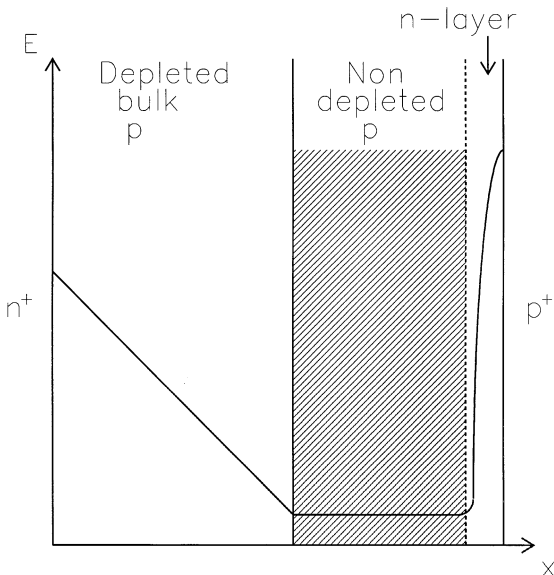


Fig. 5. A schematic diagram of the electric field pattern inside an irradiated silicon detector deduced from this work.

where μ_e and τ_e are the electron mobility and trapping time constant and w is the detector thickness. The CCE has three contributions. The first is from the charge movement in the high field region at the p^+ electrode; the second arises from the charge drifting through the non-depleted region; the third comes from the drift of the charge through the depleted region. The total CCE is then given by adding these three contributions allowing for the attenuation of the charge due to trapping. Neglecting the width of the high field region at the p^+ electrode, it can be shown that this model gives

$$\begin{aligned} \text{CCE} = & C_0 + \varepsilon_1 \lambda d (1 - \exp(-(1-d)/\lambda d)) \\ & + d \varepsilon_2 \varepsilon_1 \exp(-(1-d)/\lambda d). \end{aligned} \quad (3)$$

Here the parameter C_0 represents the first contribution. Making the simplest assumption, it was taken to be a constant independent of d . The parameter ε_1 represents the fraction of the total charge which enters the non-depleted region. In a general way, it describes the overall attenuation of the initial ionisation during the plasma time (see above). The parameter ε_2 represents the ratio of the mean charge drifting through to the charge entering into the depleted region. Thus, it describes the trapping during the charge collection in the depleted region. As discussed in Section 2.1 this trapping can be considered constant independent of d . The exponential factors in Eq. (3) arise from the loss of charge caused by trapping in the non-depleted region.

The smooth curve in Fig. 1b shows a fit of this simple model with $C_0, \varepsilon_1, \varepsilon_2$ and λ as free parameters. The model fits the data well (mean deviation of the points from the curve is 0.45%) suggesting that the assumptions made in deriving it are probably reasonable. The best-fit parameters are $C_0 = 0.4 \pm 2.1\%$, $\varepsilon_1 = 0.85 \pm 0.31$, $\varepsilon_2 = 0.59 \pm 0.19$ and $\lambda = 0.23 \pm 0.03$ where the errors are derived from the deviations of the points from the curve. The fits made for the other irradiated detectors (see Section 1) gave similar results.

The optimal value for C_0 is compatible with zero within the error and its 95% confidence level upper limit is 4.4%. Neglecting trapping along the α particle track in the high field region near the p^+ elec-

trode we can write $C_0 \sim f x_{\text{hf}}^2 / R w$, where x_{hf} is the thickness of the high field region. Here f is a calculable factor (~ 0.8) which accounts for the non-uniform ionisation deposition along the α particle track and R is the range of the α particles (20 μm in our case). This gives a rough estimate of the thickness of the high field region $x_{\text{hf}} \sim 5.5 \pm 7.9 \mu\text{m}$ indicating that it is much smaller than the detector thickness.

The physical origin of this strong field could be the existence of a thin n-type layer adjacent to the p^+ electrode. Such a possibility was already proposed some time ago [11,12]. Recent current pulse shape measurements in heavily irradiated diodes [13] also indicate the presence of a high field region near the p^+ electrode.

To reproduce the smooth growth of the CCE from the p^+ side with U_b the model described by Eq. (3) requires the existence of a non-zero electric field in the part of the bulk between the depleted area and the high field layer near the p^+ electrode (see Fig. 5). This should allow electrons released near the p^+ surface to drift in a finite time to the depleted area from where they are quickly transported to the n^+ electrode. The high mobility of the electrons drifting from the p^+ electrode helps to make this penetration fast enough for detection of the charge within the 70 ns integration time used in our electronics.

6. Conclusions

Signals from α particles and MIPs have been investigated in heavily irradiated silicon detectors. The data indicate that in a partially depleted detector the electric field falls to near zero from the n^+ side just as it should for a uniform space charge in the depleted region. However, the effect of the irradiation is to create a strong, short-range, local field, in the vicinity of the p^+ electrode so that fast α particle signals from this side are observed even when the detectors are far from being fully depleted. A small but non-zero electric field in the “non-depleted” part of the detector is also necessary to explain the data. A simple parameterisation of the CCE for this case based on this electric field pattern has been developed.

Acknowledgements

We thank S.M. Holt for his excellent technical assistance. We also thank G. Lutz, B.K. Jones, R. Richter and K.F. Smith for helpful and stimulating discussion.

References

- [1] B.K. Jones et al., Nucl. Instr. and Meth. A 395 (1997) 81.
- [2] H.-J. Ziock et al., Nucl. Instr. and Meth. A 342 (1994) 96.
- [3] L.J. Beattie et al., Nucl. Instr. and Meth. A 412 (1998) 238.
- [4] F. Lemeilleur et al., IEEE Trans. Nucl. Sci. NS- 39 (1992) 551.
- [5] Z. Li, H.W. Kraner, IEEE Trans. Nucl. Sci. NS- 38 (1991) 244.
- [6] S. Ramo, IRE 27 (1939) 584.
- [7] R.N. Williams, E.M. Lawson, Nucl. Instr. and Meth. 120 (1974) 261.
- [8] L.J. Beattie et al., Carrier lifetimes in heavily irradiated Si diodes, Nucl. Instr. and Meth. A, to be published.
- [9] C.M. Lederer, J.M. Hollander, I. Perlman, Table of Isotopes, Wiley, New York, 1968.
- [10] A. Chilingarov, T. Sloan, Proc. of the III Int. Workshop on GaAs and Related Compounds, San Miniato, World Scientific, Singapore, March 21–24 1995, p. 52.
- [11] Z. Li, H.W. Kraner, Journal of Electron. Mater. 21 (1992) 701.
- [12] R. Wunstorf, Ph.D Thesis, DESY FH1K-92-01.
- [13] Z. Li, H.W. Kraner, IEEE Trans. Nucl. Sci. NS- 43 (1996) 1590.